in various ternary systems. We have also seen how these equations and the diagram can be applied to check experimental data. The great wealth of experimental results which have been published since the first introduction of the valence-electron rules for adamantane-structure compounds a quarter of a century ago happily does not require any modifications of the valence-electron rules. On the contrary, deviating experimental results have eventually always been shown to be incorrect.

We acknowledge the help of Ms Birgitta Künzler and Ms Christine Boffi with the preparation of the drawings and the text. The part of the work performed in Geneva was supported by the Swiss National Science Foundation under contract 20-28490.90. One of the authors (PP) gratefully acknowledges support by the 'Fonds der Chemischen Industrie'.

References

BARDELEBEN, H. J. VON (1986). *Sol. Cells*, **16**, 381–390.
BOEHNKE, U. C. & KÜHN, G. (1987). *J. Mater. Sci.* **22**, 1635–1641.
BOK, L. D. C. & DE WIT, J. H. (1963). *Z. Anorg. Allg. Chem.* **324**, 162–167.
DEISEROTH, H. J., KLUGE, C. P. & PFEIFER, H. (1990). *Acta Cryst.* A**46**, C-289.
HANEMAN, D. (1988). *CRC Crit. Rev. Solid State Mater. Sci.* **14**, 377–413.
HEYDING, R. D. & MACLAREN MURRAY, R. (1976). *Can. J. Chem.* **54**, 841–848.
HÖNLE, W., KÜHN, G. & BOEHNKE, U. C. (1988). *Cryst. Res. Technol.* **23**, 1347–1354.
HÖNLE, W., KÜHN, G. & BOEHNKE, U. C. (1989). *J. Mater. Sci.* **24**, 2483–2487.
JORDAN, A. S., VON NEIDA, A. R., CARUSO, R. & KIM, C. K. (1974). *J. Electrochem. Soc.* **121**, 153–158.
KOKTA, M., CARRUTHERS, J. R., GRASSO, M., KASPER, H. M. & TELL, B. (1976). *J. Electron. Mater.* **5**, 69–89.
KONEŠOVA, T. I., BABYCINA, A. A. & KALINNIKOV, V. T. (1982). *Izv. Akad. Nauk SSSR Neorg. Mater.* **18**, 1483–1486.
LIKFORMAN, A., CARRÉ, D. & HILLEL, R. (1978). *Acta Cryst.* B**34**, 1–5.
MASSÉ, G. & REDJAI, E. (1986). *J. Phys. Chem. Solids*, **47**, 99–104.
MOOSER, E. & PEARSON, W. B. (1959). *Acta Cryst.* **12**, 1015–1022.
NEUMANN, H. (1983). *Cryst. Res. Technol.* **18**, 901–906.
PALATNIK, L. S., KOMNIK, YU. F. & ROGACOVA, O. I. (1964). *Ukr. Fiz. Zh.* **9**, 862–867.
PARTHÉ, E. (1967). *Intermetallic Compounds*, edited by J. WESTBROOK, ch. 11, pp. 180–196. New York: John Wiley.
PARTHÉ, E. (1987). *Ternary and Multinary Compounds*, edited by S. K. DEB & A. ZUNGER, pp. 3–17. Pittsburgh: Materials Research Society.
PARTHÉ, E. (1990). *Elements of Inorganic Structural Chemistry, a Course on Selected Topics*, 100 pp. Petit-Lancy, 49 Chemin du Gué, Switzerland: K. Sutter Parthé Publisher.
PHILLIPS, J. C. (1981). *Structure and Bonding in Crystals*, Vol. 1, edited by M. O'KEEFFE & A. NAVROTSKY, ch. 2, pp. 13–24. New York: Academic.
RADAOUTSAN, S. I. (1964). *Physique des Semiconducteurs, Comptes Rendus du 7e Congres International*, pp. 1177–1184. Paris: Dunod.
RIVET, J., LARUELLE, P., FLAHAUT, J. & FICHET, R. (1970). *Bull. Soc. Chim. Fr.* pp. 1667–1670.
VILLARS, P., MATHIS, K. & HULLIGER, F. (1989). *The Structures of Binary Compounds*, Vol. 2, edited by F. R. DE BOER & D. G. PETTIFOR, ch. 1, pp. 1–103. Amsterdam: North-Holland.
WUENSCH, B. J., TAKEUCHI, Y. & NOWACKI, W. (1966). *Z. Kristallogr.* **123**, 1–20.
ZAHN, G. & PAUFLER, P. (1988). *Cryst. Res. Technol.* **23**, 499–507.
ZUNGER, A. (1981). *Structure and Bonding in Crystals*, Vol. 1, edited by M. O'KEEFFE & A. NAVROTSKY, ch. 5, pp. 73–135. New York: Academic.

Acta Cryst. (1991). B**47**, 891–899

A Low-Temperature Structural Phase Transformation in CuAgS

BY CHRISTOPHER L. BAKER AND FRANK J. LINCOLN*

Department of Chemistry, University of Western Australia, Nedlands, Western Australia 6009, *Australia*

AND ANDREW W. S. JOHNSON

Electron Microscopy Centre, University of Western Australia, Nedlands, Western Australia 6009, *Australia*

(*Received* 20 *May* 1991; *accepted* 8 *July* 1991)

Abstract

The symmetry and crystal structure of CuAgS have been examined by electron and X-ray diffraction between 13 and 298 K. The room-temperature space group has been deduced by convergent-beam electron diffraction to be $Cmc2_1$ (No. 36). A second-order phase transition has been found to occur at approximately 250 K and below the transition the space group is $Pmc2_1$ (No. 26). The structures at 298 and ~120 K have been refined by single-crystal X-ray diffraction and the Rietveld method has been used to refine the structure at 13 K from powder

* To whom correspondence should be addressed.

0108-7681/91/060891-09$03.00

X-ray diffraction data. The room-temperature structure [$M_r = 203{\cdot}48$, $a = 4{\cdot}059\ (2)$, $b = 6{\cdot}617\ (4)$, $c = 7{\cdot}967\ (2)$ Å, $V = 213{\cdot}97\ (20)$ Å^3, $Z = 4$, $D_x = 6{\cdot}32$ g cm^{-3}, λ(Mo $K\alpha$) = 0·71069 Å, $\mu = 196$ cm^{-1}, $F(000) = 368$, $T = 298$ K, $R = 0{\cdot}061$, $wR = 0{\cdot}059$ for 278 reflections] is based on distorted hexagonal close packing of S atoms. The Cu atoms lie in trigonal coordination coplanar with the hexagonally packed sulfur layers. These layers are bridged by two-coordinate Ag atoms, which have large and highly anisotropic thermal motion and are bonded with near linear geometry to sulfur. The structure at ~120 K [$a = 4{\cdot}0470\ (4)$, $b = 6{\cdot}5920\ (7)$, $c = 7{\cdot}9300\ (8)$ Å, $V = 211{\cdot}56\ (4)$ Å^3, $Z = 4$, $D_x = 6{\cdot}39$ g cm^{-3}, λ(Mo $K\alpha$) = 0·71069 Å, $\mu = 198$ cm^{-1}, $F(000) = 368$, $R = 0{\cdot}036$, $wR = 0{\cdot}033$ for 736 reflections] differs in that the copper–sulfur sheets have become buckled and the Ag atoms are ordered into sites either side of the point about which they were vibrating at room temperature. The structure at 13 K, resulting from the Rietveld refinement [$a = 4{\cdot}0431\ (2)$, $b = 6{\cdot}5910\ (3)$, $c = 7{\cdot}9149\ (4)$ Å, $V = 210{\cdot}92\ (3)$, $Z = 4$, $D_x = 6{\cdot}41$ g cm^{-3}, λ(Cu $K\alpha$) = 1·54056 Å, $R_{wp} = 0{\cdot}057$, $R_B = 0{\cdot}027$] is not significantly different from that at ~120 K.

Introduction

The compound CuAgS has long been known to occur in nature. It was first analysed by Stromeyer in 1816 (Schwartz, 1935) and has since been known as stromeyerite. Early work on CuAgS was of a mineralogical nature. Interest focused both on its relationship with argentite, Ag_2S, and chalcocite, Cu_2S, and on its role as a silver-bearing mineral in silver-bearing copper ores (Schwartz, 1935; Suhr, 1955; Djurle, 1958). More recently CuAgS has been the subject of attention owing to its unusual physical properties. Above ~366 K it is an ionic conductor for both copper and silver ions, although the results of Skarda, Wuensch & Prince (1981) suggest that silver is more mobile than copper. CuAgS is grey–black in appearance with a metallic lustre and is soft and can be distorted by grinding. Frueh (1955) classed CuAgS as a semi-metal and suggested that the bonding was likely to be partially metallic. The room-temperature structure of CuAgS was earlier found to be orthorhombic with space group *Cmcm* (No. 63) or $Cmc2_1$ (No. 36) (Frueh, 1955). The structure was poorly solved in *Cmcm* with an *R* factor of 0·30.

Stromeyerite exists over the composition range $Cu_{1+x}Ag_{1-x}S$, $0{\cdot}00 \le x \le 0{\cdot}07$, and up to a cation-disordering phase transition at 366 K (Skinner, 1966). Above 366 K CuAgS enters a region of solid solution, structurally based on hexagonal close packing of sulfur, which extends to Cu_2S. Skarda *et al.* (1981) refined the structure at 388 K by neutron powder diffraction and found that Ag and Cu are not completely disordered. Instead, most of the Cu atoms remain coplanar with sulfur as in the room-temperature phase. The remainder of the cations occupy the regions between the Cu/S layers in a disordered manner. Below 366 K the Ag atoms become localized in twofold coordination between the Cu/S planes.

Experimental

Specimen preparation and sources

The single-crystal X-ray data sets were collected from fragments shattered from bulk specimens of natural CuAgS from Gowganda in Ontario, Canada. This material was analysed using an Applied Research Laboratories SEMQ electron microprobe and the composition was confirmed as $Cu_{1+x}Ag_{1-x}S$, $x = 0 \pm 0{\cdot}03$. Electron and powder X-ray diffracton analyses were performed on both natural and synthetic CuAgS. The synthetic CuAgS for electron diffraction work was prepared by solid-state reaction of the binary sulfides *in vacuo* at ~570 K for one week. The product was then ground to a powder and annealed at ~345 K in N_2 for a further month. The product was identified as primarily stromeyerite by powder XRD and then examined on aluminium EM grids, at both room and liquid-nitrogen temperature, in a Philips EM 430 transmission electron microscope operating at 300 kV. Electron diffraction data were only taken from crystals whose composition had been established by energy dispersive spectrometry. Powder data for the Rietveld refinement were collected from synthetic CuAgS, prepared by mechanically alloying a stoichiometric mixture of Cu, Ag and S for 24 h in a high-energy iron and tungsten carbide ballmill. The resulting powder was annealed in an N_2 atmosphere for a month at ~345 K. The powder was sieved to a particle size of less than 50 μm and examination by transmission electron microscopy has shown that most of these particles are actually agglomerates of smaller fragments of CuAgS. Preferred orientation was therefore thought to be unlikely.

Experimental conditions for single-crystal X-ray diffraction measurements

Single-crystal X-ray data sets were collected from natural CuAgS at both ~120 K and room temperature. Suitable crystals were selected by recording oscillation photographs from small fragments mounted on glass fibres. The room-temperature data set was measured using an Enraf–Nonius CAD-4 four-circle diffractometer. A Syntex $P2_1$ diffractometer with the crystal cooled in a stream of cold nitrogen

gas was used to collect the low-temperature data. Eight standard reflections of the form 335 were recorded four times during the room-temperature data collection. The reflections (400), ($\bar{4}00$), (080), (0$\bar{8}$0), (0,0,12) and (0,0,$\bar{1}\bar{2}$) were recorded every 100 reflections and used as standards for the low-temperature data collection. Reflections that were likely to have been obstructed by the goniometer heat shield were removed using the program *SHIELD* (Kucharski, 1990). The room- and low-temperature data sets were recorded from different crystals and the experimental conditions for these two data collections are shown in Table 1. Unless otherwise mentioned, crystallographic calculations were performed using the *XTAL*3.0 suite of programs (Hall & Stewart, 1990). Scattering and dispersion factors are from *International Tables for X-ray Crystallography* (1974, Vol. IV). A Gaussian absorption correction was performed, based on crystal dimensions obtained by combining measurements from an optical goniometer and a light microscope. The interfacial angles measured on the optical goniometer were converted to face indices using the program *CADX* (Kucharski, 1990). The reflections from the optical goniometer were from shatter faces rather than crystal growth faces and, because of the highly irregular shapes of the crystals, only approximate absorption corrections were applied. Maximum crystal dimensions were 0·02 × 0·04 × 0·14 and 0·06 × 0·10 × 0·15 mm for the room-temperature and ~120 K data sets respectively. Structure refinement of room-temperaure CuAgS was performed using the positional parameters obtained by Frueh (1955) as starting positions. These parameters were also used to start the refinement of the low-temperature structure, after first being converted to their equivalent positions in $Pmc2_1$. The structures were refined on $|F|$, with $1/\sigma$ weighting, in a full-matrix least-squares procedure. Intensity standard deviations were corrected for diffractometer instability using $\sigma_I = (I_t + I_t^2 p)^{0.5}$ with $p = 4{\cdot}00 \times 10^{-4}$ and $p = 2{\cdot}03 \times 10^{-4}$ for the room-temperature and ~120 K refinements respectively.

Experimental conditions for powder X-ray diffraction measurements

X-ray powder diffraction patterns from natural and synthetic CuAgS were recorded at a range of temperatures from room temperature down to 13 K using a Rigaku diffractometer. Specimen temperature was controlled with a thermostatted liquid-helium cold stage. The structure at 13 K has been refined using a data set recorded from synthetic CuAgS. Rietveld refinement (Rietveld, 1969) was performed using a version of the program *LHPM*1 (Wiles & Young, 1981; Hill & Howard, 1986) modified to run on an IBM PC. The peak shapes in the powder pattern were modelled using the Pearson VII function (Young & Wiles, 1982). The atom positions resulting from the ~120 K single-crystal refinement were used as starting parameters for the refinement. Refinement was begun with a few cycles on background and scale, lattice parameters and other non-positional parameters were then released. Atom positions were refined next, and finally all parameters were allowed to refine simultaneously. To improve the likelihood that the refinement had converged to a global minimum, parameters were allowed to refine in different orders and with a variety of damping factors. No thermal parameters were refined for the 13 K refinement. The experimental conditions and non-structural parameters for this refinement are presented in Table 2.

Table 1. *Experimental conditions for single-crystal structure refinements*

Monochromatic Mo $K\alpha$ radiation and $2\theta/\theta$ scan mode were used.

	120 K	298 K
Maximum $(\sin\theta)/\lambda$ (Å^{-1})	0·9077	0·8047
Minimum h, k and l	−7, −11, −14	−4, −7, −8
Maximum h, k and l	7, 11, 14	6, 10, 12
Number of reflections measured	4024	292
Number of unique reflections	736	278
Number of parameters refined	37	19
Min., max. absorption correction	1·67, 2·40	1·11, 1·53
Absorption coefficients (calculated) (cm^{-1})	198	196
Extinction parameter G	0·02	0·75
Maximum standard variation (%)	5·2	1·5
Merging R factor $[\sum(I - \langle I\rangle)/\sum I]$	0·046	0·027
Maximum shift/e.s.d. in last cycle	0·013	0·056
Min., max. in ΔF synthesis (e Å^{-3})	−3·2, 3·9	−2·7, 1·7
R (all reflections)	0·036	0·061
wR (all reflections)	0·033	0·059
S	1·260	2·392

Table 2. *Experimental conditions and non-structural parameters for the* 13 K *powder refinement*

Sample	CuAgS (synthetic)
Peak-shape parameter*	$\gamma_1 = 1{\cdot}9004$
Peak FWHM parameters	$U = 0{\cdot}260$
	$V = 0{\cdot}000$
	$W = 0{\cdot}036$
Asymmetry parameter	0·743
Angular range (2θ)	16–90
R_B (%)	2·71
R_p (%)	4·36
R_{wp} (%)	5·74

* For the Pearson VII function (Young & Wiles, 1982). The agreement indicators R_B, R_p and R_{wp} are as defined by Wiles & Young (1981). The backgound was modelled and refined using the function $y_{ib}(c) = \sum_{m=1}^{4} B_m(2\theta)^m$.

Results and discussion

The reflection conditions observed in electron diffraction patterns recorded from several zones confirm that the space group is either *Cmcm* or $Cmc2_1$,

as deduced by Frueh (1955). A convergent-beam diffraction pattern from the [010] zone is displayed in Fig. 1(*a*). This has the symmetry *m*, consistent with $Cmc2_1$ (*International Tables for X-ray Crystallography*, 1983, Vol. A). Alternatively, the diffraction-group allocation of *m*1*R* (Buxton, Eades, Steeds & Rackham, 1976), and point-group tabulation (Tanaka, Saito & Sekii, 1983) show the point group to be *mm*2 rather than *mmm*. The *m* symmetry of the $[0\bar{2}1]$ zone pattern, Fig. 1(*b*), is also consistent with $Cmc2_1$ in the projection approximation of CBED symmetry determination. Thus the structure is non-centrosymmetric, polar in the c^* direction.

Electron diffraction examination of CuAgS at liquid-nitrogen temperature was originally motivated by a desire both to reduce beam damage and to enhance the quality of the diffraction patterns. However, diffraction patterns recorded at this temperature showed reflections additional to those observed at room temperature. Further investigation has confirmed that at low temperature CuAgS undergoes a phase transition to a lower-symmetry structure. For convenience and following the accepted notation for silver iodide, the low-temperature phase will from now on be denoted γ-CuAgS, the room-temperature phase, β-CuAgS, and the cation-conducting high-temperature phase, α-CuAgS.

Figs. 2(*a*) and 2(*b*) are electron diffraction patterns taken at room temperature and 90 K respectively from the [010] zone. These patterns indicate that the *C*-centred cell extinction condition (manifest at this zone as *h*0*l*: $h = 2n$ allowed) is lost at the low-temperature phase transition and that the space group changes from $Cmc2_1$ to its maximal non-isomorphic subgroup $Pmc2_1$. Also of note in Fig. 2 are the streaks of diffuse scattering running along the a^* direction in the room-temperature pattern.

Reflections unique to the space group of the γ-phase have been observed to remain visible as the cold-stage temperature was raised from 90 to 230 K, but drift of the cold stage may have prevented their observation above 230 K. The temperature of the transition has been estimated to be 250 ± 5 K by plotting the intensity of γ-phase reflections from X-ray powder patterns against temperature and extrapolating to the temperature at which their intensity drops to zero. These intensities were obtained at 13, 80, 150, 180, 210, 220, 230 and 240 K.

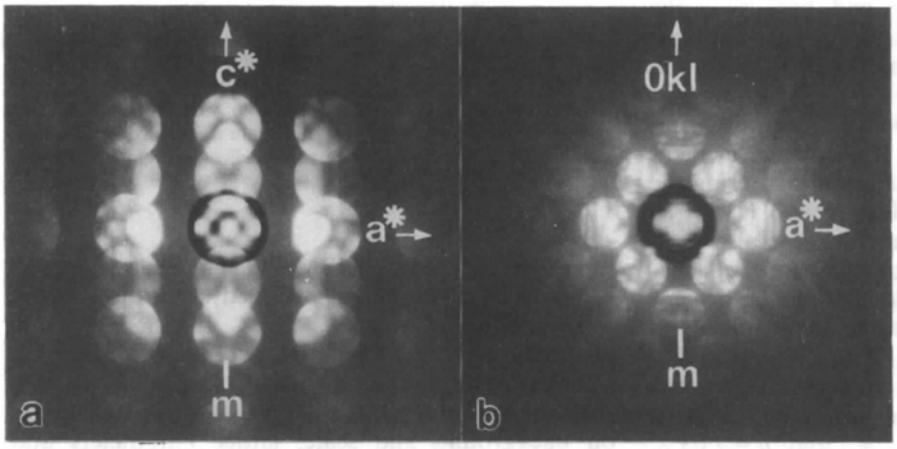

Fig. 1. Convergent-beam electron diffraction patterns recorded at room temperature from (*a*) the [010] zone, and (*b*) the $[0\bar{2}1]$ zone. Both patterns display 2*mm* symmetry in the bright-field disk but only a single mirror, perpendicular to a^*, in the zero-order zone. The patterns were recorded from two crystals and the orientation of the polar axis is unknown in each case.

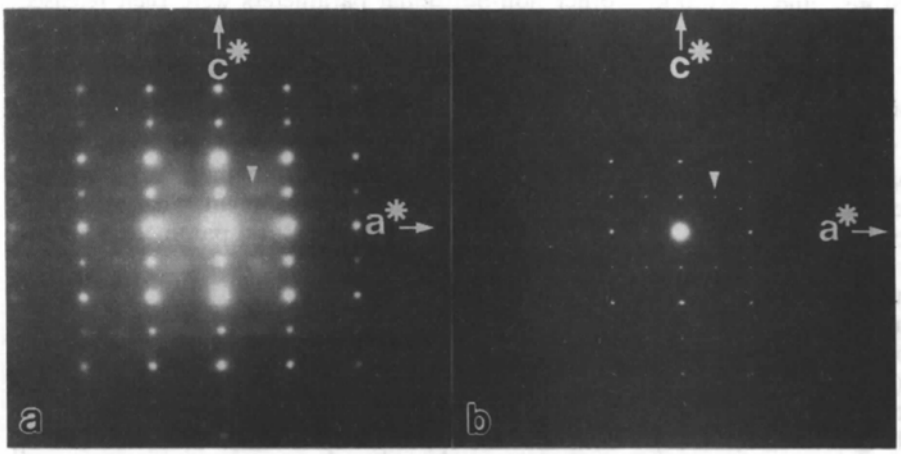

Fig. 2. Electron diffraction patterns from the [010] zone: (*a*) at room temperature, and (*b*) at 90 K. In (*a*) streaks of diffuse scattering run across the forbidden *h*0*l*: $h = n$ (odd) reflection positions. Sharp reflections occur at these positions in (*b*).

The additional reflections unique to the space group of the γ-phase were found for all samples examined at 90 K. However, some of the low-temperature patterns also contained reflections indicating that further changes to the structure sometimes occur. The reflections which index as $\frac{11}{22}l$ at the $[\bar{1}10]$ zone in Fig. 3(*b*) suggest ordering in the *ab* plane, and the occurrence of weak $00l$: $l = n$(odd) reflections at the [010] zone in Fig. 4 indicates either ordering or a further loss of symmetry along the *c* direction. EDS measurements from both ordered and adjacent regions suggest that these symmetry reductions may be composition dependent.

The primary features of the β-CuAgS structure are the same as those proposed by Frueh in 1955. The structure is based on distorted hexagonal close packing of S atoms. The Cu atoms lie in trigonal coordination in the hexagonally packed sulfur layers. These layers are bridged by two-coordinate silvers bonded with near linear geometry to S atoms in the copper–sulfur layers. A projection of the structure is displayed in Fig. 5 and the positional and thermal parameters resulting from the refinement are presented in Table 3. A significant feature of the structure is the large and highly anisotropic thermal motion of the Ag atoms. The maximum amplitude of their vibration is in the *bc* plane, perpendicular to the S—Ag—S bond direction. Attempts to refine the structure with silver disordered with 50% occupancy either side of the silver site resulted in a lower residual, although still with high thermal motion for silver. However, in the light of the results of the refinement using low-temperature data, the structure is more realistically described by high thermal motion rather than static disorder. The success of the disordered model does indicate that the harmonic approximation is a poor model of the thermal motion and that the motion of silver would be better described using an anharmonic model. The γ-CuAgS structure, Fig. 6, is closely related to that of the β-phase and both the rapidity and reversibility of the transition, and the similarity of the structures suggest that the transition is a second-order order–disorder transition. The major differences between the structures are that the thermal motion of silver is greatly diminished and that the copper–sulfur sheets buckle slightly in the low-temperature phase. As the thermal motion of the Ag atoms decreases they order into sites either side of the point about which they were vibrating in the room-temperature structure. The positional and thermal parameters resulting from this refinement are presented in Table 4(*a*).

The positional parameters resulting from the room-temperature crystal structure refinement are close to positions allowed in the centrosymmetric space group *Cmcm* and attempts to refine the structure in this space group were only slightly less successful than in $Cmc2_1$. Attempts to refine the γ-phase structure meaningfully in *Pmcm* (*Pmma*, No. 51) were unsuccessful.

The Rietveld refinement of the CuAgS structure at 13 K produced results very similar to those from the ~120 K single-crystal refinement. The parameters resulting from this refinement are tabulated in Table 4(*b*) and the observed and calculated powder patterns are presented in Fig. 7. Note that the estimated standard deviations from the Rietveld refinement should not be directly compared with those from the single-crystal refinement. It has been suggested that Rietveld e.s.d.'s can be unreliable and should be viewed critically (Post & Bish, 1989).

The coordination environments for silver in β- and γ-CuAgS are shown in Figs. 8(*a*) and 8(*b*). Silver is in twofold coordination in both phases. The two-coordinate site is produced by distortion of the octahedral interstitial sites in the sulfur packing. This distortion appears to have been produced by shearing displacement of the sulfur layers along the *b* direction. In the room-temperature phase this increases the distance to the four equatorial S atoms

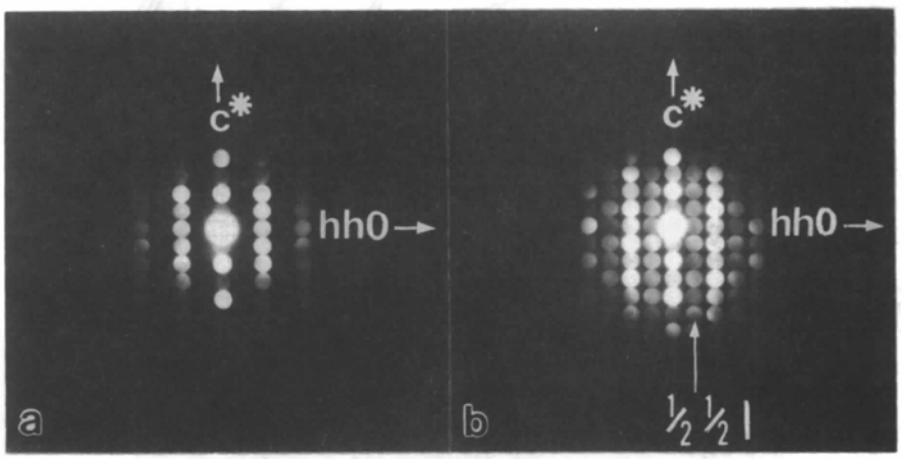

Fig. 3. Electron diffraction patterns from the $[\bar{1}10]$ zone at 90 K. The pattern in (*a*) is typical of the γ-phase. Occasionally, however, patterns as in (*b*) were observed with reflections of the form $\frac{11}{22}l$ indicative of ordering in the *ab* plane.

to ~3·4 Å and reduces the silver–apical sulfur distance to ~2·4 Å. At the transition from β- to γ-CuAgS the distance between Ag and two of the more distant S atoms decreases from 3·39 (1) to 3·262 (3) Å. This change in contact distance places silver in a highly disorted tetrahedral environment with respect to the S atoms. The S—Ag—S bond angle in γ-CuAgS is ~160°.

Both the β- and γ-phases exhibit short Ag—Cu distances, of approximately 2·9 Å, and the γ-phase also contains zigzag chains of Ag atoms running down the *a* direction with 3·25 Å Ag—Ag distances.

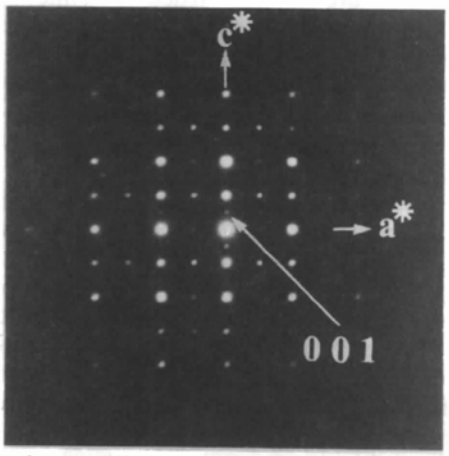

Fig. 4. An electron diffraction pattern from the [010] zone at 90 K. Reflections of the form $h0l$: $l = n$ (odd) were occasionally observed and are suggestive of either ordering in the *c* direction or further symmetry reduction from that of the γ-phase.

Table 3. *Positional and anisotropic thermal parameters resulting from the* 298 K *refinement* (*e.s.d.'s in parentheses*)

	Site (symmetry)	x	y	z
Ag1	4(*a*) (*m*)	½	0·495 (2)	¼*
Cu1	4(*a*) (*m*)	0	0·4328 (3)	0·2486 (11)
S1	4(*a*) (*m*)	½	0·2859 (6)	0·2484 (15)

	U_{11}	U_{22}	U_{33}	U_{23}
Ag1	3·60 (8)	14·4 (3)	3·61 (9)	−4·83 (12)
Cu1	1·57 (8)	3·14 (12)	3·33 (12)	−1·0 (2)
S1	1·35 (12)	1·56 (14)	3·2 (2)	−0·0 (3)

* Fixed to define origin. The anisotropic displacement exponent is of the form $-2\pi(U_{11}h^2a^{*2} + \ldots + 2U_{23}klb^*c^*)$, where U_{ij} are in Å^2 and have been multiplied by 100.

These short contact distances, combined with the metallic physical properties of CuAgS, suggest that metal–metal interaction may be important in the structure. Selected interatomic distances and angles for the β- and γ-phases are tabulated in Table 5.* The metallic character of CuAgS may be interpreted in terms of the covalency of the metal–sulfur bonding. The accessible energy of the sulfur 3*d* orbitals, combined with sulfur's large size, high polarizability and relatively low electronegativity, serve to enhance the covalency of the metal–sulfur bonding. This can, in turn, reduce the formal charge on the metal

* Lists of structure factors, and bond lengths and angles have been deposited with the British Library Document Supply Centre as Supplementary Publication No. SUP 54392 (19 pp.). Copies may be obtained through The Technical Editor, International Union of Crystallography, 5 Abbey Square, Chester CH1 2HU, England.

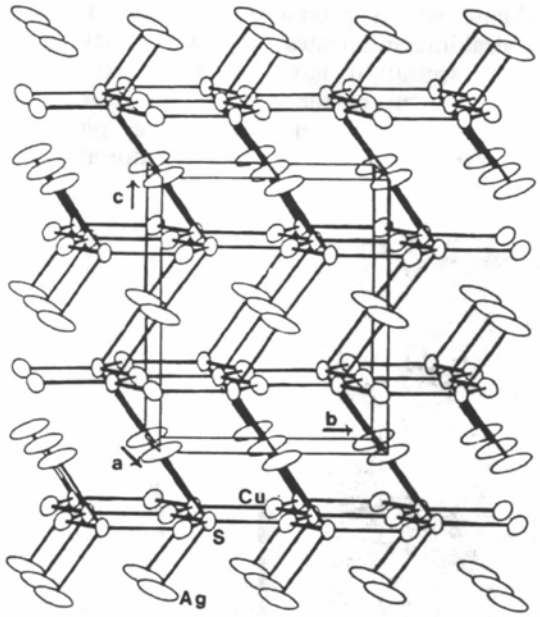

Fig. 5. The structure of CuAgS at room temperature. Thermal motion is displayed with 50% probability thermal envelopes.

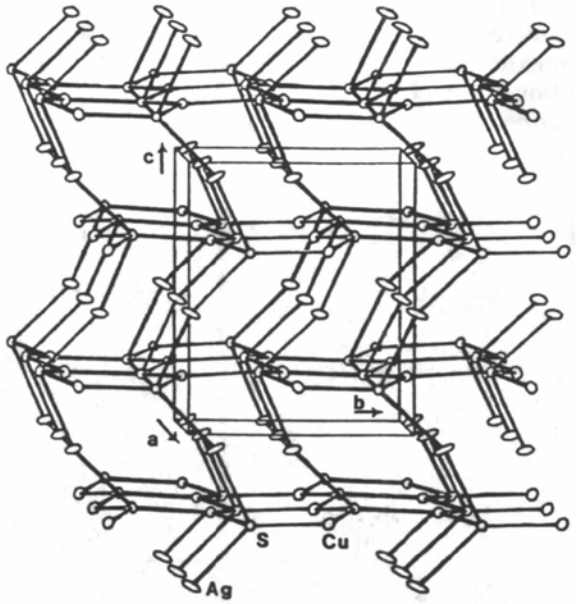

Fig. 6. The structure of CuAgS at ~120 K. Thermal motion is displayed with 50% probability thermal envelopes.

Table 4. *Positional and anisotropic thermal parameters resulting from the refinements (e.s.d.'s in parentheses)*

(*a*) 120 K refinement

	Site (symmetry)	*x*	*y*	*z*
Ag1	2(*a*) (*m*)	1	−0·0560 (2)	½*
Ag2	2(*b*) (*m*)	½	0·4402 (2)	0·9728 (1)
Cu1	2(*a*) (*m*)	1	0·5674 (2)	0·7297 (3)
Cu2	2(*b*) (*m*)	½	0·0663 (2)	0·7424 (3)
S1	2(*a*) (*m*)	1	0·2161 (4)	0·7215 (5)
S2	2(*b*) (*m*)	½	0·7133 (4)	0·7594 (5)

	U_{11}	U_{22}	U_{33}	U_{23}
Ag1	1·03 (3)	3·22 (5)	1·17 (5)	−1·38 (4)
Ag2	1·38 (4)	2·33 (4)	0·77 (4)	0·37 (4)
Cu1	0·55 (5)	1·07 (5)	1·22 (8)	0·13 (6)
Cu2	0·58 (5)	0·88 (5)	0·94 (8)	0·06 (6)
S1	0·38 (8)	0·58 (8)	0·85 (12)	0·02 (9)
S2	0·56 (9)	0·73 (8)	0·92 (13)	−0·09 (9)

(*b*) Positional parameters resulting from the Rietveld refinement using data from synthetic CuAgS at 13 K

	Site (symmetry)	*x*	*y*	*z*
Ag1	2(*a*) (*m*)	1	−0·056 (1)	½*
Ag2	2(*b*) (*m*)	½	0·427 (1)	0·9636 (8)
Cu1	2(*a*) (*m*)	1	0·569 (3)	0·720 (5)
Cu2	2(*b*) (*m*)	½	0·075 (3)	0·738 (5)
S1	2(*a*) (*m*)	1	0·202 (5)	0·712 (6)
S2	2(*b*) (*m*)	½	0·722 (5)	0·768 (6)

* Fixed to define origin.

cations and promote metal–metal bonding (Jellinek, 1988). The structure of eucairite, CuAgSe, has several interesting similarities to the stromeyerite structure. The structure is composed of near-planar layers of silver atoms combined with slabs of Cu and Se (Frueh, Czamanske & Knight, 1957). The Se atoms are arranged as sheets of squashed corner-sharing tetrahedra. The Cu atoms lie within these tetrahedra, not at their centres, but rather in near-twofold coordination close to one of their edges.

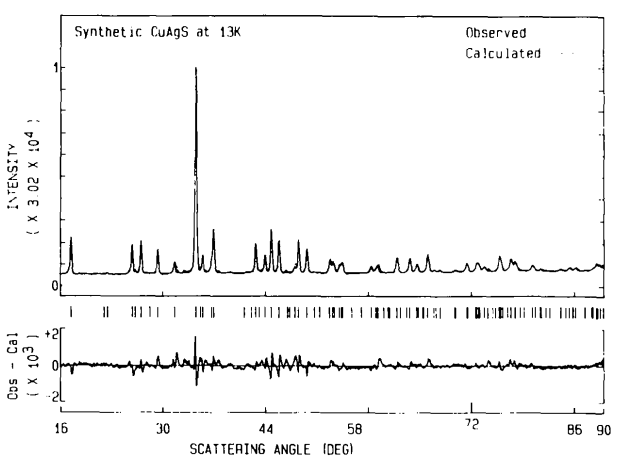

Fig. 7. Observed, calculated and difference X-ray powder diffraction profiles for CuAgS at 13 K. The vertical lines above the difference profile indicate the angles at which Bragg peaks may occur.

Silver is closely bonded to only one selenium, but is within 3·0 Å of four other Ag atoms. The shortest Ag—Cu distance is ~3·0 Å. These distances, combined with its metallic physical properties, suggest that metal–metal interaction is also important in eucairite.

There are several similarities between the CuAgS structures and the Ag_2S phases acanthite and argentite. Argentite is the high-temperature phase of Ag_2S and is based on cations disordered through a body-centred cubic sulfur array (Cava, Reidinger & Wuensch, 1980). When Ag_2S is cooled below 450 K it adopts the acanthite structure which is a superstructure based upon slightly distorted body-centred-

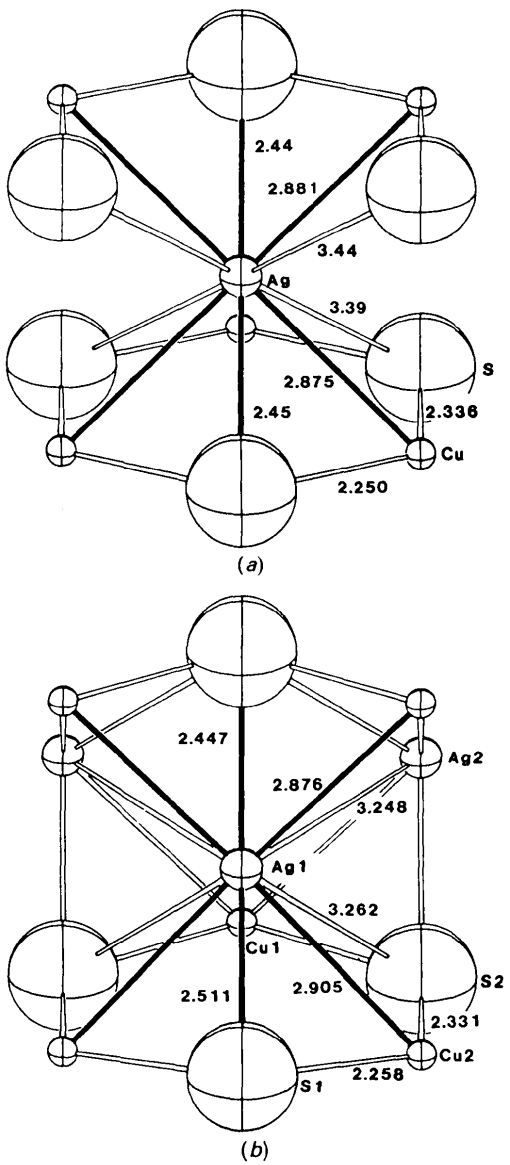

Fig. 8. The coordination environment of silver in (*a*) β-CuAgS (298 K), and (*b*) γ-CuAgS (~120 K). Distances are in Å.

Table 5. *Selected interatomic distances* (Å) *and angles* (°) (*e.s.d.'s in parentheses*)

300 K	
Ag—S	2·44 (1), 2·45 (1), 3·39 (1), 3·44 (1)
Cu—S	2·250 (2), 2·336 (5)
Ag—Cu	2·875 (7), 2·881 (7)
Ag—Ag	3·88 (2)
S—Ag—S	178·5 (6)
S—Cu—S	115·6 (1), 128·8 (2)
~120 K	
Ag1—S1	2·511 (4), 2·447 (4)
Ag2—S2	2·471 (4), 2·488 (4)
Ag1—S2	3·262 (3), 3·583 (3)
Ag2—S1	3·201 (3), 3·622 (3)
Cu1—S1	2·317 (3)
Cu2—S2	2·331 (3)
Cu1—S2	2·253 (2)
Cu2—S1	2·258 (2)
Ag1—Cu1	3·079 (2)
Ag2—Cu2	3·068 (2)
Ag1—Cu2	2·876 (2), 2·905 (2)
Ag2—Cu1	2·872 (2), 2·920 (2)
Ag1—Ag2	3·248 (2)
S1—Ag1—S1	159·9 (1)
S2—Ag2—S2	157·2 (1)
S1—Cu1—S2	115·44 (7)
S2—Cu1—S2	127·8 (1)
S1—Cu2—S1	127·3 (1)
S1—Cu2—S2	116·17 (6)

cubic sulfur packing. The Ag atoms in acanthite occupy two different environments, one of them in twofold coordination midway between two S atoms. This two-coordinate silver is close to the centre of a distorted octahedral site in the near body-centred-cubic sulfur packing of acanthite. The two nearer S atoms are at 2·47 and 2·51 Å, with four more at an average distance of 3·43 Å. The other silver has distorted tetrahedral coordination, lying almost in the planes of the S atoms (Sadanaga & Sueno, 1967).

Twofold silver coordination, present in both CuAgS and Ag_2S, is a frequently observed geometry about silver and has been explained by the relatively small energy difference between the filled *d* orbitals and the unfilled *s* orbital, which permits extensive hybridization of the d_{z^2} and *s* orbitals (Cotton & Wilkinson, 1980). The near-isostructural phases prousite (Ag_3AsS_3) and pyragyrite (Ag_3SbS_3) have much in common with γ-CuAgS. Their structures are based on pyramidal AsS_3 or SbS_3 groups joined through the S atoms to twofold, almost linearly coordinated silver atoms to form spiral like Ag—S chains. The sulfur to silver bond distance is 2·40 Å, with an S—Ag—S bond angle of ~165° (Harker, 1936).

The S—Ag—S bond angle in γ-CuAgS is also similar to the bond angle about silver in AgSCN. The basic unit of the structure is an infinite chain —Ag—S—C—N—Ag—, with an N—Ag—S bond angle of ~164·5°. There also appears to be an Ag—S interaction between the chains, with distances of 3·0 and 2·89 Å (Lindqvist, 1957).

The structural changes in CuAgS also show some similarity to the low-temperature phase transformation observed in covellite, CuS (Fjellvåg, Grønvold, Stølen, Andresen, Müller-Käfer & Simon, 1988). The structures of covellite and stromeyerite share, as a common structural element, layers of trigonally coordinated copper and sulfur. In stromeyerite the layers are bridged by Ag atoms whereas in covellite the layers are bridged by slabs of CuS_4 tetrahedra joined by S—S bonds. However, in both compounds the major change resulting from the phase transformation is a change in the coordination geometry of the cations in the region between the Cu/S layers.

We are indebted to Dr Allan Pring, Curator of Minerals at the South Australian Museum, who provided the mineral stromeyerite, and to Mr J. Hester, Dr E. N. Maslen and Professor A. H. White, of the Crystallography Centre at the University of Western Australia, for helping with the single-crystal X-ray data collection. We thank Professor T. Kajitani for the use of the low-temperature powder diffraction facilities at the Institute for Materials Research, Tohoku University, Sendai, Japan. One of us (CLB) wishes to acknowledge the financial assistance of an Australian Postgraduate Research Award.

References

BUXTON, B. F., EADES, J. A., STEEDS, J. W. & RACKHAM, G. M. (1976). *Philos. Trans. R. Soc. London*, **281**, 171–194.

CAVA, R. J., REIDINGER, F. & WUENSCH, B. J. (1980). *J. Solid State Chem.* **31**, 69–80.

COTTON, F. A. & WILKINSON, G. (1980). *Advanced Inorganic Chemistry*, 4th ed. Brisbane: John Wiley.

DJURLE, S. (1958). *Acta Chem. Scand.* **12**, 1427–1436.

FJELLVÅG, H., GRØNVOLD, F., STØLEN, S., ANDRESEN, A. F., MÜLLER-KÄFER, R. & SIMON, A. (1988). *Z. Kristallogr.* **184**, 111–121.

FRUEH, A. J. (1955). *Z. Kristallogr.* **106**, 299–307.

FRUEH, A. J., CZAMANSKE, G. K. & KNIGHT, CH. (1957). *Z. Kristallogr.* **108**, 389–396.

HALL, S. R. & STEWART, J. M. (1990). Editors. *XTAL3.0 Reference Manual.* Univs. of Western Australia, Australia, and Maryland, USA.

HARKER, D. (1936). *J. Chem. Phys.* **4**, 381–390.

HILL R. J. & HOWARD, C. J. (1986). Australian Atomic Energy Commission Report No. M112. AAEC (now ANSTO), Lucas Heights Research Laboratories, New South Wales, Australia.

JELLINEK, F. (1988). *React. Solids*, **5**, 323–339.

KUCHARSKI, E. (1990). Personal communication. Department of Chemistry, Univ. of Western Australia, Nedlands, WA 6009, Australia.

LINDQVIST, I. (1957). *Acta Cryst.* **10**, 29–32.

POST, J. E. & BISH, D. L. (1989). *Modern Powder Diffraction*, edited by D. L. BISH & J. E. POST, pp. 277–305. Washington, DC: Mineralogical Society of America.

RIETVELD, H. M. (1969). *J. Appl. Cryst.* **2**, 65–71.

SADANAGA, R. & SUENO, S. (1967). *Mineral. J. Jpn*, **5**, 124–143.

SCHWARTZ, G. M. (1935). *Econ. Geol.* **30**, 128–146.

SKARDA, C., WUENSCH, B. J. & PRINCE, E. (1981). *NBS Tech. Note* 1160, pp. 57–63.
SKINNER, B. J. (1966). *Econ. Geol.* **61**, 1–26.
SUHR, N. (1955). *Econ. Geol.* **50**, 347–350.
TANAKA, M., SAITO, R. & SEKII, H. (1983). *Acta Cryst.* A**39**, 357–368.
WILES, D. B. & YOUNG, R. A. (1981). *J. Appl. Cryst.* **14**, 149–151.
YOUNG, R. A. & WILES, D. B. (1982). *J. Appl. Cryst.* **15**, 430–438.

Acta Cryst. (1991). B**47**, 899–904

Neutron Diffraction at 115 K to 1·09 Å^{-1} from Cobalt Phthalocyanine

BY PHILIP A. REYNOLDS, BRIAN N. FIGGIS AND EDWARD S. KUCHARSKI
School of Chemistry, University of Western Australia, Nedlands, WA 6009, *Australia*
AND SAX A. MASON
Institut Laue–Langevin, BP 156*X*, 38042 *Grenoble, France*

(*Received* 20 *May* 1991; *accepted* 26 *July* 1991)

Abstract

$[Co(C_{32}H_{16}N_8)]$, $M_r = 571{\cdot}47$, monoclinic, $P2_1/c$, $a = 14{\cdot}489\ (9)$, $b = 4{\cdot}763\ (4)$, $c = 19{\cdot}156\ (16)$ Å, $\beta = 120{\cdot}76\ (4)^\circ$, $V = 1136\ (3)$ Å^3, $Z = 2$, $D_n = 1{\cdot}67$ Mg m^{-3}, neutron $\lambda = 0{\cdot}753\ (1)$ Å, $\mu = 0{\cdot}0879$ mm^{-1}, $F(000) = 46{\cdot}05 \times 10^{-14}$ m, $T = 115{\cdot}0\ (1)$ K, $R(F) = 0{\cdot}018$, $R(F^2) = 0{\cdot}030$, $S = 1{\cdot}08$ for 2789 reflections, 1008 at wavevectors above 0·7 Å^{-1}, with anharmonic Gram–Charlier expansion refinement and thermal diffuse-scattering (TDS) correction derived from theoretical intermolecular potentials. The introduction of 715 cubic and quartic anharmonic parameters reduces $R(F^2)$ by 0·011 and S by 0·11 from the values obtained in a harmonic refinement. Use of the local molecular approximate symmetry is not helpful in describing anharmonicity. Quartic parameters are more significant than cubic ones. Much of the anharmonic correction seems to result from intermolecular interaction affecting the relatively soft motion along **b**, resulting in one-particle potential wells with flat bottoms along **b**, but relatively harmonic potential in the *ac* plane. Agreement of positional parameters with the 115 K X-ray charge-density results is good, if similar refinements are made. But the neutron thermal parameters are significantly lower than X-ray, 8% on average, probably reflecting a difference in the TDS correction in the two experiments. The molecule is significantly distorted from planarity.

Introduction

Cobalt phthalocyanine (Fig. 1), CoPc, has interesting electronic properties with biological implications (Buchler, 1987; Dolphin, 1979). Both X-ray (Figgis, Kucharski & Reynolds, 1989*a*, and references therein) and polarized neutron (Williams, Figgis & Mason, 1981) diffraction experiments have been performed to examine the charge and spin densities. Reynolds & Figgis (1991) have analysed these and other metal(II) phthalocyanine diffraction and theoretical results to elucidate the ground electronic states in the crystals.

The 115 K charge-density X-ray study could not be interpreted in terms of a simple harmonic model for nuclear motion together with a valence-electron density model. This raised the question of the extent of anharmonicity and the accuracy of the positional and thermal parameters derived from the X-ray data, considerations which are critical in any modelling of valence-electron density.

In this paper we describe a neutron diffraction experiment, at the same temperature as the X-ray diffraction experiment, and which extends further in reciprocal space than is usual – up to the limit of the X-ray experiment. It allows an examination of anharmonic effects and of the reliability of X-ray-defined thermal parameters.

Experimental

Data collection

The crystal was from the same batch, grown by entrainer vacuum sublimation techniques, as used in previous diffraction experiments. The crystal was cut from that employed in the 4·3 K neutron diffraction experiment (Williams, Figgis, Mason, Mason & Fielding, 1980) and was a 6·0 mm needle along **b**, with an irregular eight-sided cross section [(100), (10$\bar{1}$), (10$\bar{2}$), (00$\bar{1}$), ($\bar{1}$00), ($\bar{1}$01), ($\bar{1}$02), (001)] of maxi-

0108-7681/91/060899-06$03.00